

Geometric PID-type attitude tracking control on $SO(3)$

Hossein Eslamiat, Ningshan Wang, Amit K. Sanyal

Department of Mechanical and Aerospace Engineering, Syracuse University, Syracuse, NY 13244, USA

Abstract

This article develops and proposes a geometric nonlinear proportional-integral-derivative (PID) type tracking control scheme on the Lie group of rigid body rotations, $SO(3)$. Like PD-type attitude tracking control schemes that have been proposed in the past, this PID-type control scheme exhibits almost global asymptotic stability in tracking a desired attitude profile. The stability of this PID-type tracking control scheme is shown using a Lyapunov analysis. A numerical simulation study demonstrates the stability of this tracking control scheme, as well as its robustness to a disturbance torque. In addition, a numerical comparison study shows the effectiveness of the proposed integrator term.

Keywords: Geometric control, Lie groups, Lyapunov stability

1. Introduction

Classical PID control schemes are widely used in practice and have several applications due to their ease of design and tunable properties. PID controllers create a control input based on a tracking error, which is the difference between the actual output and a desired (reference) output. This control input has three terms: one proportional to the error, one proportional to the time integral of the error, and another term proportional to the time derivative of the error. Using PID feedback has the advantage of eliminating steady state error (using an integral term) and reducing oscillations (using a derivative term) [1]. In addition, when the mathematical model of a plant is not known and hence analytical design methods cannot be used, PID controllers prove to be very useful [2]. The popularity of PID controllers can be attributed partly to their good performance in a wide range of operating conditions and partly to their functional simplicity [3]. Some PID controllers have been proposed for rigid body attitude tracking by utilizing local coordinates or quaternions, such as the ones in [4, 5, 6, 7], however, these suffer from singularities or unwinding [8]. Unwinding occurs when in response to certain initial conditions, a closed loop trajectory undergoes a homoclinic-like orbit that initiates near the desired attitude equilibrium. For more details on unwinding, see [9, 10].

Geometric mechanics is the interface for applying geometric control to mechanical systems. This approach results in conserving features of the configuration space without the need of local coordinates or parameterization. An early work extending classical PD control to mechanical systems evolving on configuration manifolds is [11], where PD-type control was used to stabilize a desired configuration. It is worth noting that controls

for such systems are defined on the tangent space of the configuration manifold. In subsequent years, others have proposed various geometric PD-type controllers, such as in [12, 13, 14, 15]. If there is a bounded parameter error or disturbance, a geometric PD controller can guarantee global boundedness of tracking errors, although, they might not converge to zero. By choosing sufficiently large PD gains, the errors can be made arbitrarily small. However this can result in amplifying undesirable noise, saturating actuators, and requiring large control effort. This, alongside the added robustness, motivates adding an integrator to a PD type controller.

Research on geometric PID-type control includes [16], in which the authors consider control of a mechanical system on a Lie group. They propose an integral action, evolving on the Lie group, to compensate the drift resulting from a constant bias in velocity and torque inputs. However, they assume a constant time-invariant bias, and only discuss feedback stabilization and not the feedback tracking problem. The work in [17] defines an integral term by putting the derivative of integral error equal to the intrinsic gradient of the error function *plus* a velocity error term. However, since the derivative of the integral term is not on the tangent space, the integrator is nonintrinsic. Therefore, the integrator depends on the coordinates chosen for the Lie algebra of the Lie group, unlike the intrinsic PID controller proposed in [18]. A more recent work [19] considers the tracking problem and proposes a PID controller for a rigid body with internal rotors. This builds on the previous PID controller designed in [18], where it is shown an intrinsic (geometric) integral action ensures that tracking errors converge to zero, in response to constant velocity commands. Following up on this prior work, [19] develops an intrinsic PID controller on $SO(3)$ for attitude tracking applications. The proposed PID-type controller and tracking algorithm can work in conjunction with trajectory generation algorithms such as in [20, 21, 22, 23, 24, 25, 26]. A generated trajectory can be considered as the desired trajectory

Email addresses: heslamia@syr.edu (Hossein Eslamiat),
nwang16@syr.edu (Ningshan Wang), aksanyal@syr.edu (Amit K. Sanyal)

and be tracked by the algorithm presented in this paper.

This paper is organized as following. Section 2 formulates the problem by introducing coordinate frames used, reference attitude trajectory and attitude dynamics. Section 3 discusses tracking error kinematics and dynamics. Section 4 proposes the geometric PID controller, along with its stability proof. Section 5 is dedicated to a Lie group variational integrator (LGVI) discretization and numerical validation, and comparison with a PD type controller and discussion of disturbance-free case. Finally, section 6 concludes the paper and gives directions for future work.

2. Problem Formulation

The treatment in this paper is general and can be applied to vehicles modeled as rigid bodies, e.g., spacecraft, unmanned underwater vehicles and unmanned aerial vehicles like quadrotors.

2.1. Coordinate frames

The two coordinate systems used to define the attitude of a rigid body are inertial and body-fixed coordinates. Attitude of the vehicle is defined as the rotation from body-fixed frame to inertial frame and is denoted $R \in \text{SO}(3)$. For attitude tracking, we also define a desired attitude trajectory in time, denoted $R_d(t)$. In addition, we denote by Ω the angular velocity and Ω^d denotes the desired angular velocity.

2.2. Reference Attitude Generation

The desired attitude trajectory for the rigid body is assumed to be generated and available a priori. As an example for rotorcraft unmanned aerial vehicles (UAVs) the desired attitude trajectory can be generated from the position trajectory, by using the known dynamics model and actuation. Let m and J denote mass and inertia of a rigid body, respectively. The rotational dynamics of the rigid body is given by:

$$\dot{R} = R\Omega^\times, \quad (1)$$

$$J\dot{\Omega} = J\Omega \times \Omega + \tau, \quad (2)$$

where τ is the input torque and the cross map: $(\cdot)^\times : \mathbb{R}^3 \rightarrow \text{SO}(3)$ is given by [27]:

$$x^\times = \begin{bmatrix} x_1 \\ x_2 \\ x_3 \end{bmatrix}^\times = \begin{bmatrix} 0 & -x_3 & x_2 \\ x_3 & 0 & -x_1 \\ -x_2 & x_1 & 0 \end{bmatrix}.$$

3. Tracking error kinematics and dynamics on TSO(3)

The attitude tracking error is defined by [27]:

$$Q = R_d^T R. \quad (3)$$

Taking the time derivative results in:

$$\begin{aligned} \dot{Q} &= \dot{R}_d^T R + R_d^T \dot{R} = (R_d(\Omega^d)^\times)^T R + R_d^T R \Omega^\times \\ &= R_d^T R \Omega^\times - (\Omega^d)^\times R_d^T R = Q\Omega^\times - (\Omega^d)^\times Q \\ &= Q(\Omega - Q^T \Omega^d)^\times = Q\omega^\times, \end{aligned} \quad (4)$$

where $\omega = \Omega - Q^T \Omega^d$ is the angular velocity tracking error. As a result,

$$\begin{aligned} J\dot{\Omega} &= J \frac{d}{dt}(\omega + Q^T \Omega^d) = J(\dot{\omega} + \dot{Q}^T \Omega^d + Q^T \dot{\Omega}^d) \\ &= J(\dot{\omega} + (Q\omega^\times)^T \Omega^d + Q^T \dot{\Omega}^d) \\ &= J(\dot{\omega} + Q^T \dot{\Omega}^d - \omega^\times Q^T \Omega^d) \end{aligned} \quad (5)$$

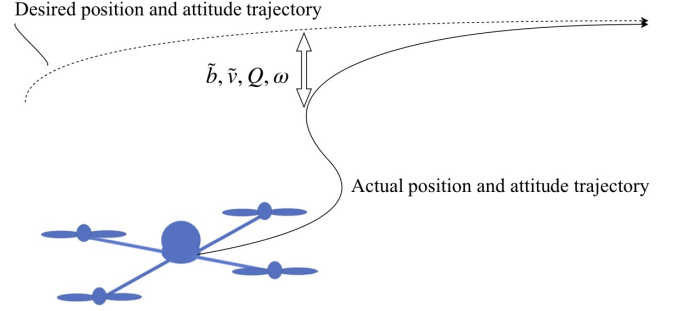


Figure 1: Tracking errors

Figure (1) shows a schematic of tracking errors for a quadrotor UAV model, as the difference between the desired trajectory and actual trajectory. In this figure, \tilde{b} denotes position tracking error and \tilde{v} denotes translational velocity tracking error, both defined in inertial frame.

4. Main Result

Lemma 1

Let $\langle X, Y \rangle$ denote $\text{tr}(X^T Y)$ and e_1, e_2, e_3 be unit vectors in x, y, z directions, respectively. Let I denote the 3×3 identity matrix and K be:

$$K = \begin{bmatrix} k_1 & 0 & 0 \\ 0 & k_2 & 0 \\ 0 & 0 & k_3 \end{bmatrix} \text{ where } k_i \text{ are distinct positive scalars,}$$

and define $S_K(Q)$ as:

$$S_K(Q) = \sum_{i=1}^3 k_i (Q^T e_i)^\times \times e_i, \quad (6)$$

such that $\frac{d}{dt} \langle K, I - Q \rangle = \omega^T S_K(Q)$. Then $\langle K, I - Q \rangle$ is a Morse function on $\text{SO}(3)$.

The proof of Lemma 1 is given in [28] and is omitted here for brevity.

Theorem 1

Let $k_P, k_D, k_I \in \mathbb{R}^+$ denote proportional, derivative and integrator feedback gains, respectively, and let $S_K(Q)$ be defined as in Lemma 1. Let $F_I \in \mathbb{R}^3 \simeq \mathfrak{so}(3)$ be the proposed integrator term given by:

$$J\dot{F}_I = -k_P S_K(Q) - k_D \omega, \quad F_I(0) = 0. \quad (7)$$

Considering attitude dynamics of a rigid body as in equations (1)-(2), then the following control law:

$$\begin{aligned} \tau = & k_I F_I - k_P S_K(Q) - k_D \omega \\ & + J(Q^T \dot{\Omega}^d - \omega^\times Q^T \Omega^d) - J\Omega \times Q^T \Omega^d, \end{aligned} \quad (8)$$

leads to asymptotically stable tracking of (R_d, Ω^d) , where (Q, ω) are tracking errors given by (3)-(4).

Proof

Let $V : \text{SO}(3) \times \mathbb{R}^3 \rightarrow \mathbb{R}^+$ be a Lyapunov candidate given by:

$$V = \bar{V} + k_p \langle K, I - Q \rangle, \quad (9)$$

where

$$\bar{V} = \frac{1}{2} \{ (F_I - \omega)^T J (F_I - \omega) + \omega^T J \omega \}. \quad (10)$$

Note that by Lemma 1, $\langle K, I - Q \rangle$ is a Morse function on $\text{SO}(3)$, so is V . By comparing equation (5) and dynamics equation (1) we get:

$$J\dot{\omega} + J(Q^T \dot{\Omega}^d - \omega^\times Q^T \Omega^d) = J\Omega \times \Omega + \tau, \quad (11)$$

then,

$$J\dot{\omega} = J\Omega \times \Omega + J(\omega^\times Q^T \Omega^d - Q^T \dot{\Omega}^d) + \tau. \quad (12)$$

As a result,

$$\omega^T J\dot{\omega} = \omega^T [J\Omega \times \Omega + J(\omega^\times Q^T \Omega^d - Q^T \dot{\Omega}^d) + \tau]. \quad (13)$$

Consider equation (9), according to Lemma 1, by taking time derivative of V we get:

$$\dot{V} = \dot{\bar{V}} + k_p \omega^T S_K(Q). \quad (14)$$

Taking time derivative of \bar{V} in equation (10) gives

$$\dot{\bar{V}} = (F_I - \omega)^T J (\dot{F}_I - \dot{\omega}) + \omega^T J \dot{\omega}, \quad (15)$$

where $J\dot{\omega}$ is as expressed in equation (12), and F_I as in equation (7). Consider equation (13), and set:

$$\begin{aligned} J\Omega \times \Omega + J(\omega^\times Q^T \Omega^d - Q^T \dot{\Omega}^d) + \tau = \\ k_I F_I + J\Omega \times \omega - k_P S_K(Q) - k_D \omega. \end{aligned} \quad (16)$$

This gives the control torque as:

$$\begin{aligned} \tau = & k_I F_I - k_P S_K(Q) - k_D \omega \\ & + J(Q^T \dot{\Omega}^d - \omega^\times Q^T \Omega^d) - J\Omega \times Q^T \Omega^d. \end{aligned} \quad (17)$$

Then as a result

$$\omega^T J\dot{\omega} = -k_P \omega^T S_K(Q) - k_D \omega^T \omega + k_I \omega^T F_I. \quad (18)$$

Using equation (18), and replacing equation (15) in (14) results in:

$$\dot{V} = -k_I F_I^T F_I + 2k_I \omega^T F_I - k_D \omega^T \omega. \quad (19)$$

By setting $k_D = k_I + k_{DI}$ where $k_{DI} > 0$, we get:

$$\dot{V} = -k_{DI} \omega^T \omega - k_I (F_I - \omega)^T (F_I - \omega) \leq 0. \quad (20)$$

Considering equations (9) and (20) and evoking the invariance-like theorem 8.4 in [29] (which uses Barbalat's lemma), we can conclude the following. As $t \rightarrow \infty$, both ω and $(F_I - \omega)$ approach 0. Therefore, as $t \rightarrow \infty$, $F_I \rightarrow 0$. In addition, we can conclude that as $t \rightarrow \infty$, $\langle K, I - Q \rangle \rightarrow 0$ and hence $Q \rightarrow I$. Therefore the tracking errors (Q, ω) converge to $(I, 0)$ in an asymptotically stable manner. This means that the proposed control law in equation (17) leads to asymptotically stable tracking of the desired attitude trajectory (R_d, Ω^d) . ■

4.1. Robustness to disturbance torque

The stability result of Theorem 1 guarantees asymptotic convergence of tracking errors (Q, ω) to $(I, 0)$ when there is no disturbance. If there exist a bounded disturbance torque D , tracking errors will converge to a bounded neighborhood of $(I, 0)$. Theorem 2 gives a specific relation between the size of a neighborhood of $(I, 0)$ and disturbance torque D , to guarantee convergence of tracking errors (Q, ω) to that neighborhood of $(I, 0)$.

Theorem 2

Let D be a disturbance torque that is bounded in norm by a scalar γ , i.e., $\|D\| \leq \gamma$, acting on the dynamics of the system given by equation (2), as follows:

$$J\dot{\Omega} = J\Omega \times \Omega + \tau + D. \quad (21)$$

Then with the control law given by equation (17), the tracking errors (Q, ω) converge to a neighborhood of $(I, 0)$ given by

$$\mathcal{N}_{(I,0)} := \{(Q, \omega) : \|(2\omega - F_I)\| \leq \gamma \leq k_{DI} \|\omega\|^2 + k_I \|F_I - \omega\|^2\}, \quad (22)$$

asymptotically in time.

Proof

By considering disturbed dynamics in equation (21) and following similar steps as in the proof of theorem 1, it can be verified that for the disturbed system \dot{V} becomes:

$$\dot{V} = -k_{DI} \omega^T \omega - k_I (F_I - \omega)^T (F_I - \omega) + (2\omega - F_I)^T D. \quad (23)$$

The $(2\omega - F_I)^T D$ term is upper bounded by

$$(2\omega - F_I)^T D \leq \|(2\omega - F_I)\| \|D\| \leq \|(2\omega - F_I)\| \gamma, \quad (24)$$

and hence, \dot{V} is upper bounded by

$$\dot{V} \leq -k_{DI} \omega^T \omega - k_I (F_I - \omega)^T (F_I - \omega) + \|(2\omega - F_I)\| \gamma. \quad (25)$$

Therefore,

$$\dot{V} \leq -k_{DI} \|\omega\|^2 - k_I \|F_I - \omega\|^2 + \|(2\omega - F_I)\| \gamma. \quad (26)$$

Consequently, \dot{V} is negative semi-definite if

$$-k_D \|\omega\|^2 - k_I \|F_I - \omega\|^2 + \|(2\omega - F_I)\| \gamma \leq 0, \quad (27)$$

and that is a sufficient condition for asymptotic convergence of (Q, ω) to the neighborhood $\mathcal{N}_{(I,0)}$. The size of this neighborhood is given by (22). ■

For numerical simulations in the next section, we introduce a time-varying disturbance and show how the proposed PID-type controller effectively compensates for disturbance, compared to a geometric PD-type controller. In addition, we compare our geometric PID-type controller with a classic "non-geometric" PID controller.

5. Numerical Simulation

For simulation purposes, we consider a quadrotor UAV. The complete control of a quadrotor UAV has two loops: the outer loop position control (translational) and the inner loop attitude control (rotational). The attitude should change such that the desired position trajectory is achieved. In this paper we are looking at the inner loop of attitude control, and proposing a geometric PID type controller for it. However, to have meaningful simulations, we would like to utilize a position controller as well, in conjunction with our proposed attitude controller. Hence for the outer loop of position, we use the translational controller in equation (18) of [30], as given below:

$$\ddot{\mathbf{f}} = e_3^T R^T (m g e_3 + P \tilde{\mathbf{b}} + L_v (R \mathbf{v} - \mathbf{v}_d) - m \dot{\mathbf{v}}_d). \quad (28)$$

To make meaningful comparisons, we use this outer loop position controller in all the following simulations, while varying the inner loop attitude controller for our comparison purposes. In addition, a desired attitude trajectory based on the quadrotor UAV's position trajectory is considered, and then tracked by the proposed algorithm. The desired position trajectory is a helix; going up in the z direction, as shown with a black dotted line in Fig. 3.

5.1. Discretization by LGVI

Discretization of equations of motion is done by utilizing a Lie Group Variational Integrator (LGVI), which, in contrast to general purpose numerical integrators, preserves the structure of configuration space without parameterization or re-projection. The LGVI scheme used in this work was first proposed in [31]. The time step for discretization is a constant $h = t_{k+1} - t_k$. Here $(\cdot)_k$ denotes a parameter of the system at time step k . The discrete equations of motions are:

$$\begin{aligned} R_{k+1} &= R_k \mathcal{F}_k, \\ \Omega_{d_{k+1}}^\times &= \frac{1}{h} \log(R_{d_k}^T R_{d_{k+1}}), \\ J \Omega_{k+1} &= \mathcal{F}_k^T J \Omega_k + h \tau_k, \end{aligned}$$

where $\mathcal{F}_k \approx \exp(h \Omega_k^\times) \in \text{SO}(3)$ is evaluated using Rodrigues' formula:

$$\mathcal{F}_k = \exp(f_k^\times) = I + \frac{\sin \|f_k\|}{\|f_k\|} f_k^\times + \frac{1 - \cos \|f_k\|}{\|f_k\|^2} (f_k^\times)^2, \quad (29)$$

where

$$f_k = h \Omega_k.$$

This guarantees that R_k evolves on $\text{SO}(3)$. For more details on discretization using LGVI please refer to [31].

5.2. Simulation Results

The quadrotor model considered in the simulations has the following physical properties:

$$J = \text{diag}(0.0820, 0.0845, 0.1377), \quad m = 4.34 \text{ kg}, \quad (30)$$

and the time step in simulations is $h = 0.01$ s. To demonstrate the performance of the proposed geometric PID-type controller, and show effectiveness of the novel integrator term, we introduce a time-varying disturbance torque to the system with components shown in Fig. 2, and then compare the results with the geometric PD-type attitude controller of [30].

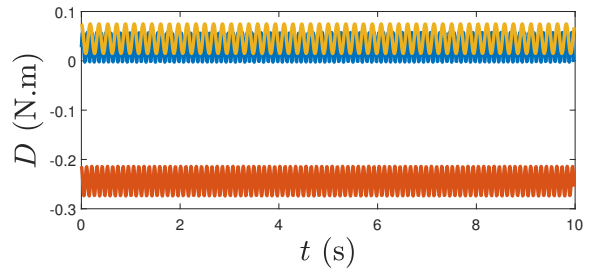


Figure 2: Components of disturbance torque D and how they change with time

The disturbance shown in the above figure consists of the sum of constant and sinusoidal terms. The simulations were done using Matlab to encode the LGVI algorithm and the control laws.

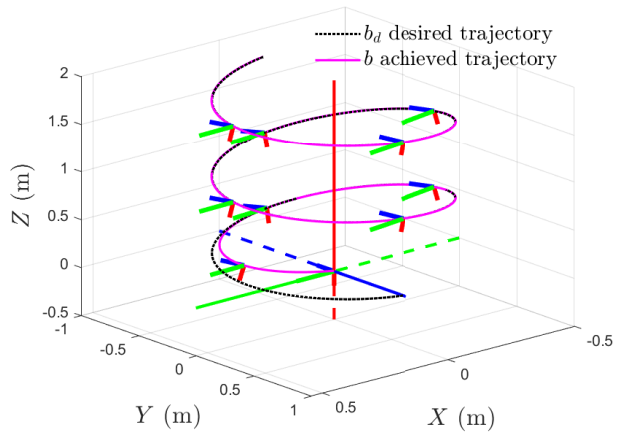


Figure 3: 3D tracking

Figure 3 shows how the position and attitude trajectories converge to the desired trajectory using the proposed PID-type attitude tracking control in conjunction with the position tracking controller in equation (28).

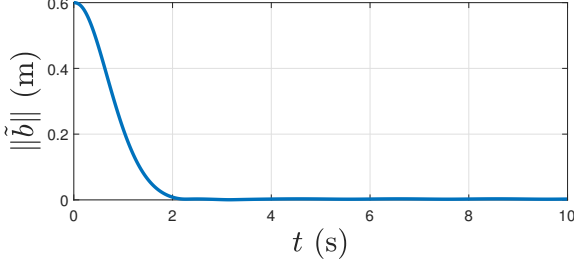


Figure 4: Position error norm vs Time

Figure 4 shows the magnitude of position tracking error over time, and how it converges to zero.

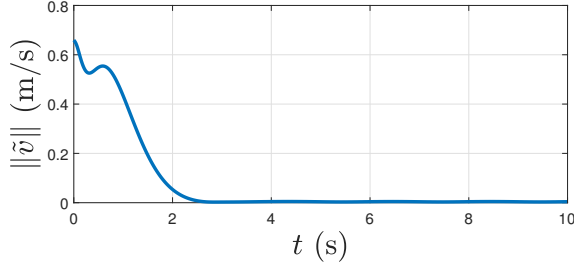


Figure 5: Velocity error norm vs Time

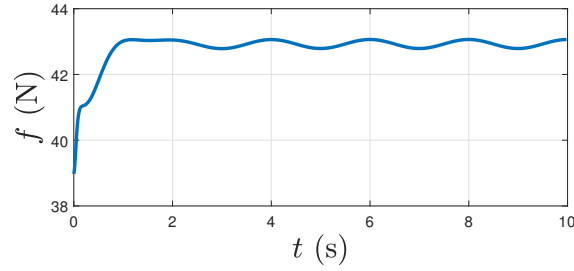


Figure 6: Thrust vs Time

Figure 5 shows associated velocity tracking error magnitude converging asymptotically to zero as expected. Figure 6 shows the thrust magnitude required to track the desired position trajectory.

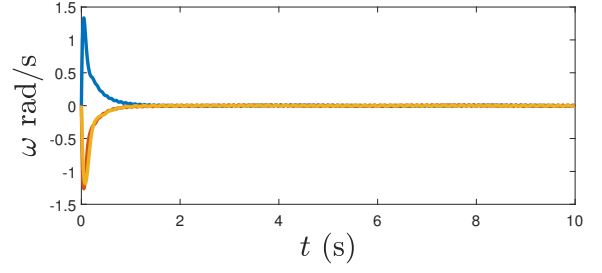


Figure 7: Angular velocity tracking error dynamics vs time

Figure 7 shows components of the angular velocity tracking error, ω , and that they converge asymptotically to zero with time.

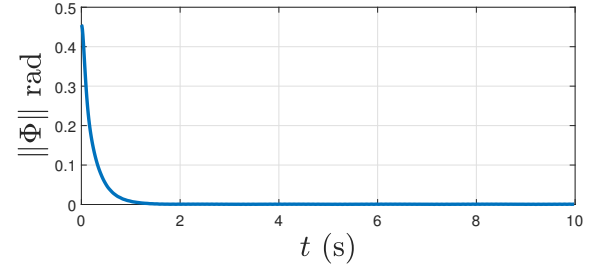


Figure 8: Attitude tracking error vs time

Figure 8 shows the asymptotic convergence of the attitude tracking error with time.

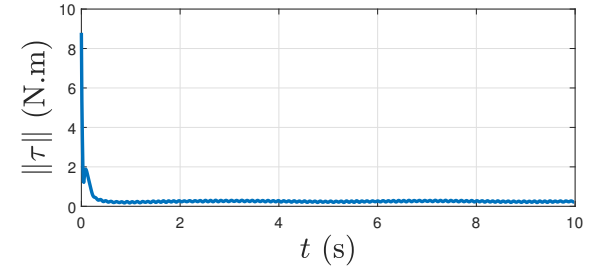


Figure 9: Magnitude of Control torque vs time

Figure 9 shows the magnitude of the proposed control torque over time.

5.3. Effectiveness of the integrator term

Effectiveness of the integrator term in the proposed geometric PID-type attitude control is shown by the following comparison:

Under the same disturbance torque of Fig. 2, we use the geometric PD-type attitude controller of [30] to track the same trajectory, and compare the results with our proposed geometric PID-type attitude controller.

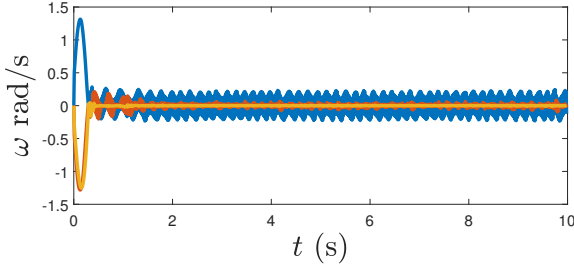


Figure 10: Angular velocity tracking error dynamics vs time for PD-type controller of [30]

Figure 10 shows that for the PD-type controller, components of ω do not converge to zero but oscillate with noticeable amplitudes about it. On comparing this figure with Fig. 7, we see that the geometric PID-type controller shows significantly better performance.

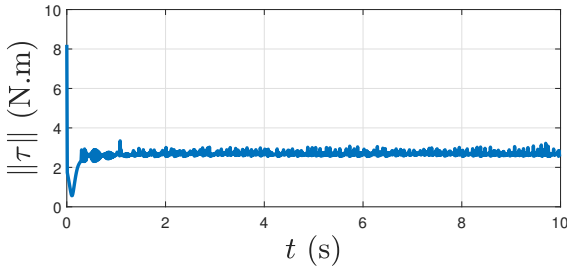


Figure 11: Magnitude of Control torque vs time for PD-type controller of [30]

Figure 11 shows rapid oscillations in control that will likely not be realizable by, and therefore should not be implemented on, a quadrotor UAV. Comparing Fig. 9 with Fig. 11, the geometric PID-type controller shows remarkably better performance with negligible oscillations. In addition, Figure 11 shows the large magnitude of the required control torque given by the geometric PD-type controller. Comparing Fig. 9 with the Fig. 11, we can see much less required control effort was needed by the geometric PID-type controller compared to the geometric PD-type controller.

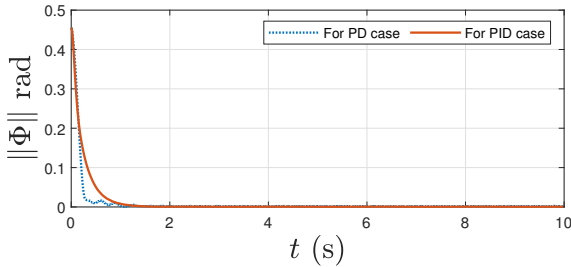


Figure 12: Norm of attitude tracking error for the proposed PID-type controller and the PD-type controller in [30]

Figure 12 shows norm of the attitude tracking error for both PD and PID-type controllers. The PID-type controller shows this error to be decreasingly more smoothly and with lesser oscillations than the PD-type controller.

Overall, the comparison in this subsection shows that the proposed PID-type controller has significant advantages over a PD-type controller in steady state performance as well as disturbance attenuation. It tracks the same maneuvering attitude trajectory better while requiring significantly less overall control effort under the influence of a time-varying disturbance torque.

5.4. Comparing with zero disturbance case

Another interesting observation can be made by comparing the performance of the proposed PID-type controller under influence of disturbance, which was presented in section 5.2, with its performance when there is no disturbance ($D = 0$), while tracking the same desired trajectory. If disturbance is zero, then the proposed PID controller, gives the following results in our numerical simulation.

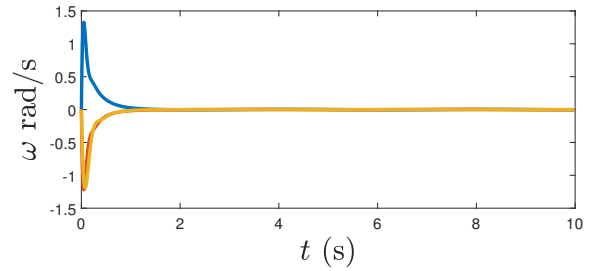


Figure 13: Angular velocity tracking error dynamics vs time for $D = 0$

Figure 13 shows components of the angular velocity tracking errors over time and that they converge asymptotically to zero. This case ($D = 0$) can be thought of as an ideal case, and by comparing Fig. 7 with the above figure, we can see how little the performance of the PID-type controller changes under the influence of disturbance. The time plots in Fig. 7 show a similar tracking profile to the ideal case of zero disturbance (Fig. 13).

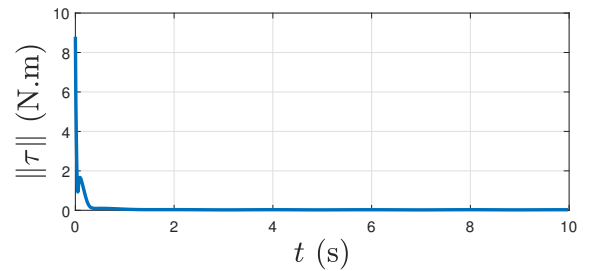


Figure 14: Magnitude of Control torque vs time for $D = 0$

Figure 14 shows the control torque magnitude, as given by the proposed PID-type controller when there is no disturbance, i.e., $D = 0$. Again considering this case as an ideal case, we see how well the PID-type controller performs in the presence of disturbance: the profile in Fig. 9 is similar (with minor oscillations) to that of Fig. 14.

To summarize, in this subsection we compared the performance of the PID-type attitude tracking controller for two situations; one when there is no disturbance torque (ideal case) and the other in the presence of a disturbance torque. We observed that under a disturbance torque the proposed controller performs well, and results in similar (but slightly degraded) performance as in the ideal case of zero disturbance.

5.5. Comparing with a classic non-geometric PID controller

In this part, we utilize a classic non-geometric PID controller given in [32] as the attitude controller. Following are the results of this simulation. As can be seen from the diverging errors, this non-geometric PID does not perform well with our LGVI dynamics engine.

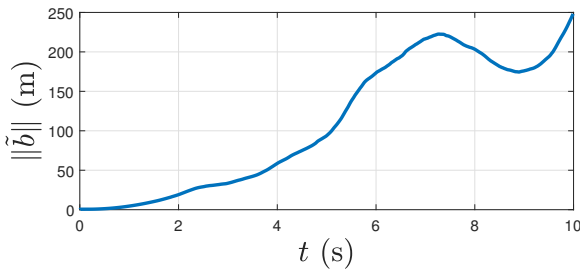


Figure 15: Position error norm vs Time for non-geometric PID

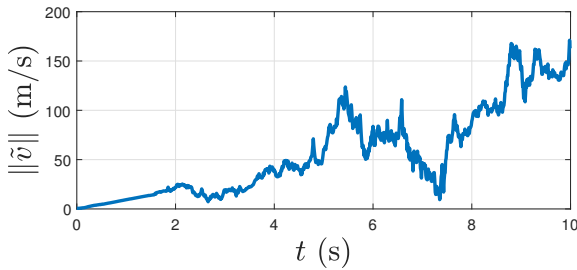


Figure 16: Velocity error norm vs Time for non-geometric PID

In Figures 15 and 16 diverging position error norm and velocity error norm are shown, respectively.

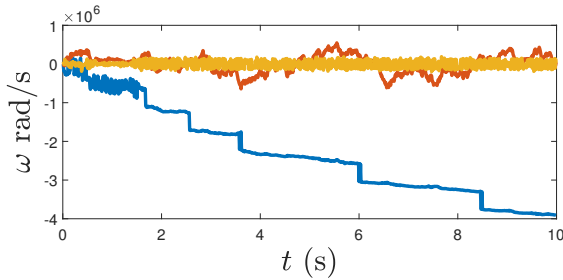


Figure 17: Angular velocity tracking error dynamics for non-geometric PID

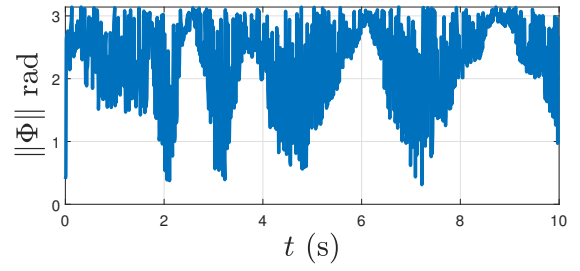


Figure 18: Attitude tracking error for non-geometric PID

Figures 17 and 18 show attitude and angular velocity tracking errors and how they perform.

From this simulation it can be inferred that the geometric PID controller performs better with the LGVI, compared to a classic non-geometric PID controller that can not enforce the errors to zero in conjunction with the position controller in equation (28).

6. Conclusion and Future Work

In this work a geometric PID-type attitude tracking control scheme was developed and its stability was shown theoretically using Lyapunov analysis on the state space of rigid body attitude motions. Analysis of robustness to disturbance torque was presented. Numerical simulations confirmed the performance of the attitude controller, even in the presence of an oscillating disturbance torque, in comparison with a geometric PD-type attitude controller, and a non-geometric PID controller. In the near future, we plan to implement this attitude control scheme in software-in-the-loop (SITL) simulations using the open source PX4 software for a particular quadrotor UAV configuration. This will be followed by hardware implementation on the corresponding UAV platform.

Acknowledgements

The authors acknowledge support from the National Science Foundation award CISE 1739748.

References

References

- [1] G. F. Franklin, D. J. Powell, and A. Emami-Naeini, *Feedback Control of Dynamic Systems*, 4th ed. Upper Saddle River, NJ, USA: Prentice Hall PTR, 2001.
- [2] K. Ogata, *Modern Control Engineering*, ser. Instrumentation and controls series. Prentice Hall, 2010. [Online]. Available: <https://books.google.com/books?id=Wu5GpNAelzkC>
- [3] R. Dorf and R. Bishop, *Modern Control Systems*. Pearson Prentice Hall, 2011. [Online]. Available: <https://books.google.com/books?id=lerbSAAACAAJ>
- [4] J. T. Wen and K. Kreutz-DeIgado, "The attitude control problem," *IEEE Transactions on Automatic Control*, vol. 36, no. 10, pp. 1148–1162, Oct 1991.
- [5] C. Li, K. L. Teo, B. Li, and G. Ma, "A constrained optimal PID-like controller design for spacecraft attitude stabilization," *Acta Astronautica*, vol. 74, pp. 131 – 140, 2012. [Online]. Available: <http://www.sciencedirect.com/science/article/pii/S009457651100381X>

- [6] J. Su and K.-Y. Cai, "Globally stabilizing proportional-integral-derivative control laws for rigid-body attitude tracking," *Journal of Guidance, Control, and Dynamics*, vol. 34, pp. 1260–1264, 07 2011.
- [7] K. Subbarao and M. Akella, "Differentiator-free nonlinear proportional-integral controllers for rigid-body attitude stabilization," *Journal of Guidance Control and Dynamics - J GUID CONTROL DYNAM*, vol. 27, pp. 1092–1096, 11 2004.
- [8] N. A. Chaturvedi, A. K. Sanyal, and N. H. McClamroch, "Rigid-body attitude control," *IEEE Control Systems Magazine*, vol. 31, no. 3, pp. 30–51, June 2011.
- [9] S. P. Bhat and D. S. Bernstein, "A topological obstruction to continuous global stabilization of rotational motion and the unwinding phenomenon," *Systems and Control Letters*, vol. 39, no. 1, pp. 63 – 70, 2000. [Online]. Available: <http://www.sciencedirect.com/science/article/pii/S0167691199000900>
- [10] C. G. Mayhew, R. G. Sanfelice, and A. R. Teel, "On path-lifting mechanisms and unwinding in quaternion-based attitude control," *IEEE Transactions on Automatic Control*, vol. 58, no. 5, pp. 1179–1191, May 2013.
- [11] D. E. Koditschek, "The application of total energy as a Lyapunov function for mechanical control systems," February 1989.
- [12] F. Bullo and R. M. Murray, "Proportional Derivative (PD) control on the euclidean group," in *proceedings of 3rd European Control Conference*, 1995.
- [13] T. Lee, M. Leok, and N. H. McClamroch, "Geometric tracking control of a quadrotor UAV on SE(3)," in *49th IEEE Conference on Decision and Control (CDC)*, Dec 2010, pp. 5420–5425.
- [14] D. H. S. Maithripala, J. M. Berg, and W. P. Dayawansa, "Almost-global tracking of simple mechanical systems on a general class of Lie groups," *IEEE Transactions on Automatic Control*, vol. 51, no. 2, pp. 216–225, Feb 2006.
- [15] R. Hamrah, R. R. Warier, and A. K. Sanyal, "Discrete-time stable tracking control of underactuated rigid body systems on SE(3)," in *2018 IEEE Conference on Decision and Control (CDC)*, Dec 2018, pp. 2932–2937.
- [16] Z. Zhang, A. Sarlette, and Z. Ling, "Integral control on Lie groups," *Systems and Control Letters*, vol. 80, pp. 9 – 15, 2015.
- [17] F. Goodarzi, D. Lee, and T. Lee, "Geometric nonlinear PID control of a quadrotor UAV on SE(3)," 07 2013, pp. 3845–3850.
- [18] D. Maithripala and J. M. Berg, "An intrinsic PID controller for mechanical systems on Lie groups," *Automatica*, vol. 54, pp. 189 – 200, 2015. [Online]. Available: <http://www.sciencedirect.com/science/article/pii/S0005109815000060>
- [19] A. Nayak, R. N. Banavar, and D. H. S. Maithripala, "Almost-global tracking for a rigid body with internal rotors," *European Journal of Control*, vol. 42, pp. 59 – 66, 2018.
- [20] M. W. Mueller, M. Hehn, and R. D'Andrea, "A computationally efficient motion primitive for quadcopter trajectory generation," *IEEE Transactions on Robotics*, vol. 31, no. 6, pp. 1294–1310, Dec 2015.
- [21] Y. Bouktir, M. Haddad, and T. Chettibi, "Trajectory planning for a quadrotor helicopter," in *2008 16th Mediterranean Conference on Control and Automation*, June 2008, pp. 1258–1263.
- [22] M. Cutler and J. How, *Actuator Constrained Trajectory Generation and Control for Variable-Pitch Quadrotors*. American Institute of Aeronautics and Astronautics, 2017/03/19 2012. [Online]. Available: <http://dx.doi.org/10.2514/6.2012-4777>
- [23] H. Eslamiat, Y. Li, N. Wang, A. K. Sanyal, and Q. Qiu, "Autonomous waypoint planning, optimal trajectory generation and nonlinear tracking control for multi-rotor uavs," in *2019 18th European Control Conference (ECC)*, June 2019, pp. 2695–2700.
- [24] D. Mellinger and V. Kumar, "Minimum snap trajectory generation and control for quadrotors," in *Robotics and Automation (ICRA), 2011 IEEE International Conference on*. IEEE, 2011, pp. 2520–2525.
- [25] B. T. Ingersoll, J. K. Ingersoll, P. DeFranco, and A. Ning, ser. AIAA AVIATION Forum. American Institute of Aeronautics and Astronautics, Jun 2016, ch. UAV Path-Planning using Bezier Curves and a Receding Horizon Approach, 0. [Online]. Available: <https://doi.org/10.2514/6.2016-3675>
- [26] Y. Li, H. Eslamiat, N. Wang, Z. Zhao, A. K. Sanyal, and Q. Qiu, "Autonomous waypoints planning and trajectory generation for multi-rotor UAVs," in *Proceedings of Design Automation for CPS and IoT*, 2019.
- [27] A. Sanyal, N. Nordkvist, and M. Chyba, "An almost global tracking control scheme for maneuverable autonomous vehicles and its discretization," *IEEE Transactions on Automatic Control*, vol. 56, no. 2, pp. 457–462, Feb 2011.
- [28] M. Izadi and A. K. Sanyal, "Rigid body attitude estimation based on the Lagrange-d'Alembert principle," *Automatica*, vol. 50, no. 10, pp. 2570 – 2577, 2014.
- [29] H. K. Khalil, *Nonlinear systems*. Prentice Hall, 2002.
- [30] S. P. Viswanathan, A. K. Sanyal, and E. Samiei, "Integrated guidance and feedback control of underactuated robotics system in SE(3)," *Journal of Intelligent and Robotic Systems*, vol. 89, no. 1, pp. 251–263, Jan 2018. [Online]. Available: <https://doi.org/10.1007/s10846-017-0547-0>
- [31] N. Nordkvist and A. K. Sanyal, "A Lie group variational integrator for rigid body motion in SE(3) with applications to underwater vehicle dynamics," in *49th IEEE Conference on Decision and Control (CDC)*, Dec 2010, pp. 5414–5419.
- [32] P. Pounds, R. Mahony, and P. Corke, "Modelling and control of a large quadrotor robot," *Control Engineering Practice*, vol. 18, no. 7, pp. 691–699, 2010.